Structural analysis of the Lützow-Holm Complex in Akarui Point, East Antarctica, and overview of the complex

Takeshi Ikeda[1]* and Tetsuo Kawakami[2]

[1] *Department of Earth and Planetary Sciences, Graduate School of Science,*
Kyushu University, 33 Hakozaki, Fukuoka 812-8581
[2] *Department of Earth Sciences, Faculty of Education, Okayama University,*
Tsushima-naka 3-chome, Okayama 700-8530
*Corresponding author. E-mail: ikeda@geo.kyushu-u.ac.jp

Abstract: Two phases of major deformation are responsible for the dominant structures at Akarui Point, Prince Olav Coast, East Antarctica. The first phase, referred to as D_{m-1}, is associated with the formation of foliation defined by biotite and hornblende aligned subparallel to compositional layering. The foliation is locally parallel to the axial planes of isoclinal and intrafolial folds of gneissic layers. Boudins are present with long axes subparallel to the axes of F_{m-1} folds. A second phase of deformation, denoted as D_m, produced a crenulation lineation and axial planar foliation that trends NW-SE throughout the area. This foliation is parallel to the axial plane of the large-scale Akarui Point Synform, which has a fold axis plunging gently SE, suggesting that the Akarui Point Synform formed during D_m. A locally-developed third phase of deformation (D_{m+1}) produced gentle folding of S_{m-1} and S_m. Chemical compositions of biotite grains that define S_{m-1} and S_m are similar. Migmatite shows close associations with D_{m-1} and D_m structures. This suggests that both phases of deformation were contemporaneous with high-grade metamorphism.

Compilation of structural data in other areas reveals that D_{m-1} and D_m controlled dominant structures of the Lützow-Holm Complex. Several folding events after D_m may be responsible for differing orientations of D_m structures between localities.

key words: structural analysis, deformation, Akarui Point, Lützow-Holm Complex

1. Introduction

The Lützow-Holm Complex is located along the Sôya and Prince Olav Coasts of Queen Maud Land, East Antarctica. Gneisses in the region were formed during a Cambrian metamorphic event with peak conditions that increased in grade westward from amphibolite facies to granulite facies. Peak metamorphic pressure increases from 6 to 11 kbar with increasing peak temperature from 680 to over 1000°C (Hiroi *et al.* 1983a, 1987; Shiraishi *et al.*, 1984, 1992, 1994; Motoyoshi *et al.*, 1989; Motoyoshi and Ishikawa, 1997; Fraser *et al.*, 2000; Yoshimura *et al.*, 2004). Rocks in the complex preserve microstructures that record a metamorphic history with a clockwise pressure (*P*)-temperature (*T*) path (Hiroi *et al.*, 1983a, b, 1986; Motoyoshi and Ishikawa, 1997; Fraser *et al.*, 2000). The *P-T* paths of individual rocks are distinct from the metamor-

phic field gradient of the complex (*e.g.*, Shiraishi *et al.*, 1987).

Structural studies of the gneisses provide important constraints on the development of these regional distribution of *P-T* conditions and *P-T* paths of the complex. Previous studies have defined several phases of deformation in the relatively high-grade section of the complex, along the coast of Lützow-Holm Bay, as briefly summarized by Kawakami and Ikeda (2004a). Yoshida (1978) characterized four phases of deformation, denoted as D_1, D_2, D_3 and D_4. He also noted pre-D_1 structures that have not been analyzed in detail, and emphasized their importance in understanding the early stage of the evolution of the complex. In contrast, only two phases of deformation have been proposed to account for outcrop patterns and fold interference patterns in the relatively low-grade section along the Prince Olav Coast (Shiraishi *et al.*, 1983; Hiroi *et al.*, 1983c).

Shiraishi *et al.* (1983) overviewed the structural features in the low- and high-grade areas of the Lützow-Holm Complex, and concluded that two major phases of deformation were responsible for the dominant structures of the complex, but they did not deal with pre-D_1 structures. Recent studies have revealed features of pre-D_1 structures that indicate deformation during or just after peak metamorphism at Skallevikshalsen (Kawakami and Ikeda, 2004a) and the Ongul Islands (M. Ishikawa *et al.*, 1994; Kawakami and Ikeda, 2004b).

The authors have analyzed structures in several localities over a wide range of metamorphic grades, including Skallevikshalsen (Kawakami and Ikeda, 2004a), the Ongul Islands (Kawakami and Ikeda, 2004b) and Akarui Point (Cape Akarui) (this study). The present paper describes macro- to microstructures at Akarui Point formed during different phases of deformation, and discusses their timing relative to the formation of large-scale folds and peak metamorphism. Combining these observations with those in other localities, we will describe the structural features of the Lützow-Holm Complex in general.

2. Outline of geology and metamorphism

Akarui Point lies on the Prince Olav Coast, East Antarctica, and corresponds to the lowest-grade part of the transitional zone between amphibolite-facies and granulite-facies sections of the Lützow-Holm Complex (Hiroi *et al.*, 1983b; Shiraishi *et al.*, 1984). The transitional zone is characterized by the sporadic occurrence of orthopyroxene and gedrite (Shiraishi *et al.*, 1984). Pressure and temperature conditions in the transitional zone were estimated as 7.2–7.5 kbar, 750°C at Tenmondai Rock, 12 km east of Akarui Point (Hiroi *et al.*, 1983b).

Akarui Point is composed mainly of biotite-hornblende mafic gneiss and felsic gneiss that contains garnet, biotite and, locally, hornblende (Fig. 1; Yanai *et al.*, 1984). Relict kyanite occurs as inclusions in garnet and plagioclase in pelitic gneisses where sillimanite is stable in the matrix (Hiroi *et al.*, 1983a). Garnet in ultramafic rocks is rimmed by symplectite composed of spinel, plagioclase and orthopyroxene (Yanai *et al.*, 1984; Hiroi *et al.*, 1986). These features have been well explained by a clockwise *P-T* path, similar to other areas of the complex, that includes a prograde transition from kyanite-stable to sillimanite-stable conditions, followed by decompression that is respon-
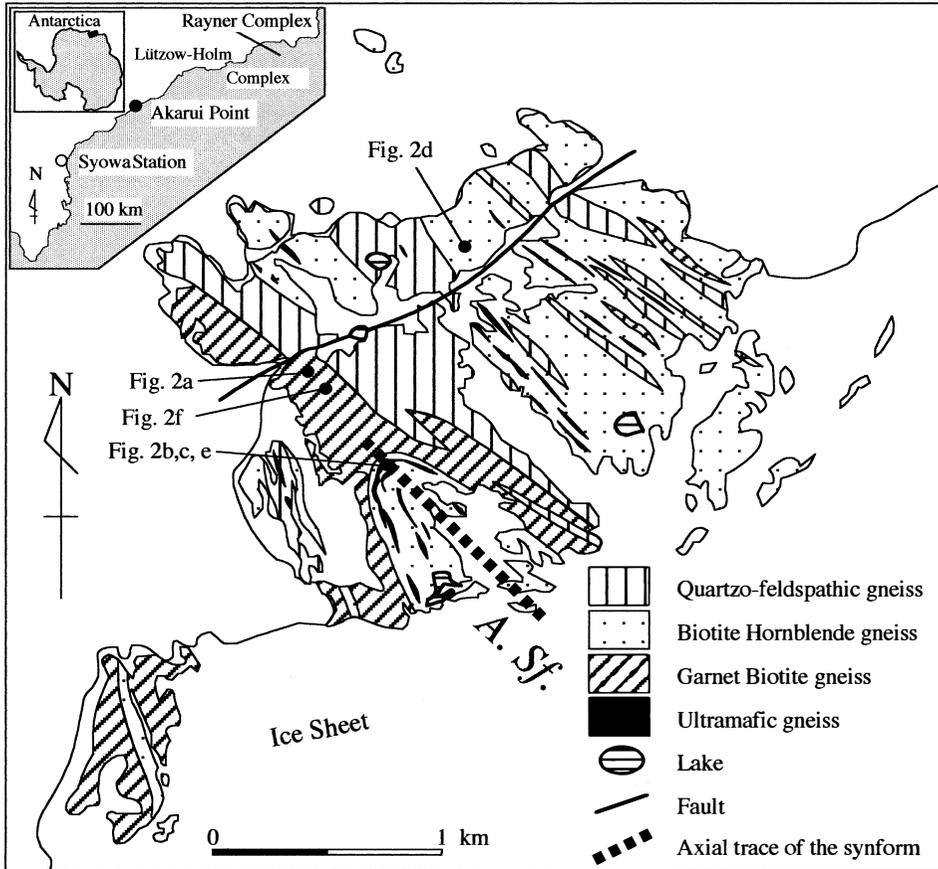
Fig. 1. Geological map of Akarui Point after Yanai et al. (1984), showing axial trace of the Akarui
Point Synform (*A. Sf.*) together with localities of outcrops described in this paper.

sible for breakdown of garnet (*e.g.*, Hiroi *et al.*, 1986). Hiroi *et al.* (1997) detected
Ca-zoning in garnet and suggested that high-temperature conditions were of relatively
short duration, so that growth zoning was not homogenized by intracrystalline diffusion.

Yanai *et al.* (1984) constructed a lithological map of the area, and recognized a
synform and two antiforms on a kilometre scale. These large-scale structures fold both
gneissic layers and mineral foliations, suggesting that the area underwent at least two
phases of deformation. We found calcite veins at the eastern ($68°27'19''$S, $41°27'53''$
E) and western ($68°27'42''$S, $41°26'11''$E) ends of the fault described by Yanai *et al.*
(1984) that trends ENE-WSW in the north of the area (Fig. 1). The veins clearly cut
granitic-pegmatitic dykes that trend oblique to the foliations in the host gneisses. No
reaction textures between the veins and the wall rocks were detected in the field,
suggesting that this fault formed under low-temperature conditions after metamor-
phism.

3. Major and minor structures

The synform described by Yanai *et al*. (1984) is easily detectable in aerial photographs (Plate 1 of Yanai *et al*., 1984), and is herein referred to as the Akarui Point Synform.   The synform has a subvertical axial plane that trends NW-SE, and the hinge contains biotite-hornblende mafic gneiss with thin ultramafic layers (Fig. 1).   On the eastern limb of the Akarui Point Synform, a mineral foliation subparallel to the axial plane strikes NW-SE and dip steeply SW.

Three phases of deformation were responsible for mesoscopic and microscopic structures, and are denoted as D_{m-1}, D_m and D_{m+1} in temporal order.

3.1. D_{m-1} structures

D_{m-1} structures include tight and intrafolial folds (F_{m-1}), boudinage and mineral foliations (S_{m-1}). S_{m-1} is defined by the preferred orientation of biotite and hornblende, subparallel to gneissic layers. S_{m-1} is axial planar to intrafolial F_{m-1} that is locally developed in pelitic gneisses (Fig. 2a). F_{m-1} plunges gently SE. S_{m-1} strikes NW-SE with steep dips towards the SW except in the hinge of the Akarui Point Synform, where it has an ENE-WSW strike and gentle dips toward the SSE (Fig. 3). Some thin melanocratic layers have been boudinaged, with neck zones filled with leucocratic rock that grades into adjacent leucocratic layers (Fig. 2b).   Most boudins are elongate parallel to compositional layers. S_{m-1} is curved into boudin necks (Fig. 2b).   At the hinge of the Akarui Point Synform, leucocratic veins trend subparallel to the later foliation (S_m, as described later) and clearly cut the boudin (Fig. 2c).   These features suggest that the boudinage is a D_{m-1} structure.   Stretching lineations defined by the preferred orientation of sillimanite and hornblende have been recognized on S_{m-1} planes.

3.2. D_m structures

D_m structures include F_m folds that re-orient compositional layers and S_{m-1}, and locally developed S_m that are axial planar to F_m folds. F_m have similar orientations to F_{m-1}, and S_m strikes NW-SE with nearly a vertical dip (Fig. 3). S_m is restricted to relatively fine-grained layers at F_m hinges (Fig. 2d).   Leucocratic veins occur parallel to F_m axial planes in the southwestern part of the area, near the axial trace of the Akarui Point Synform (Fig. 2c, e).   Crenulation lineation of S_{m-1} occurs locally parallel to F_m axes.

Orientation of S_m fluctuates considerably even in a narrow area (Fig. 3).   This feature cannot be explained by D_{m+1} deformation described below.   Competency contrast may be responsible for the scattering in orientation of the locally developed foliation.

3.3. D_{m+1} structures

A third deformation, D_{m+1}, corresponds to local and open F_{m+1} folding of D_m structures with a metre-scale wavelength (Fig. 2f).   No axial planar foliation is developed.   The occurrence of F_{m+1} is sparse. F_{m+1} have axes plunging gently SW and subvertical axial planes.
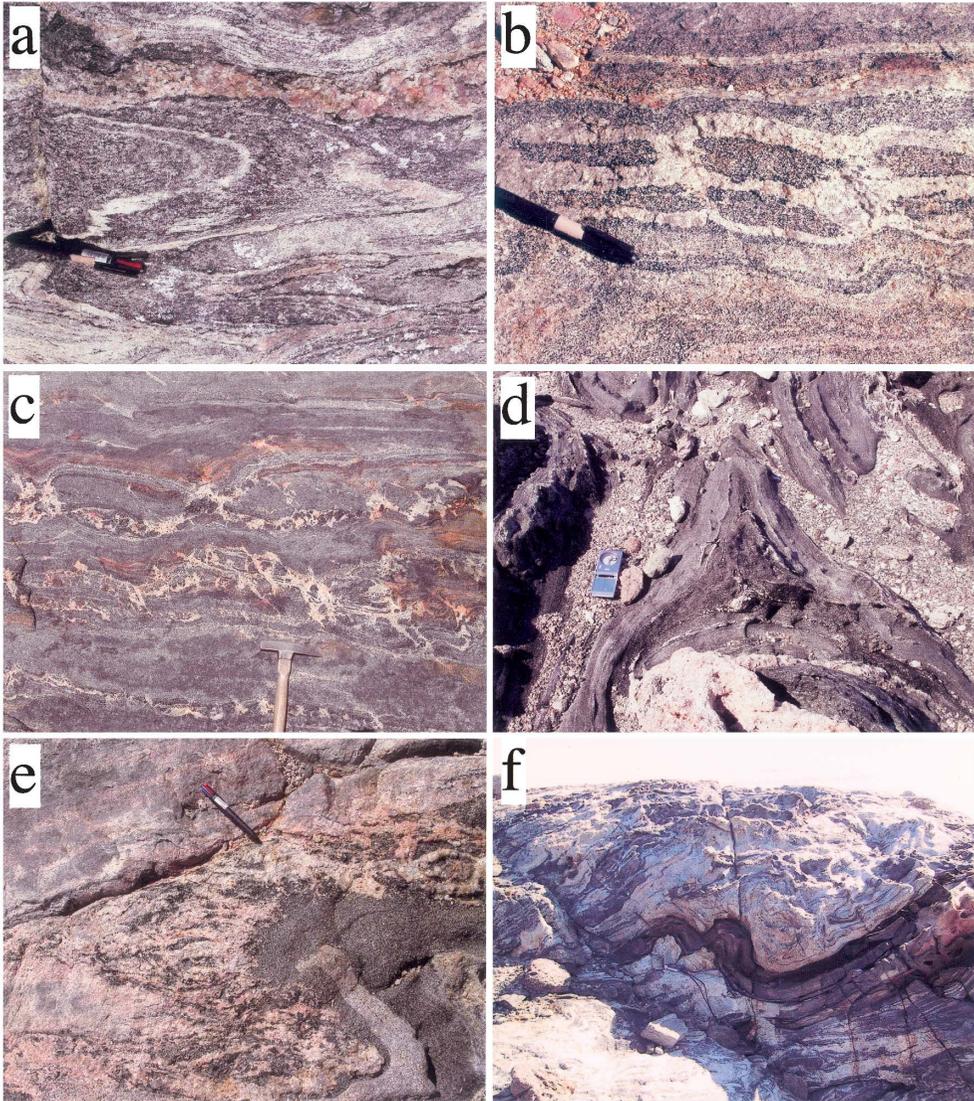
Fig. 2. *Mode of deformation of rocks at Akarui Point. a) Intrafolial folds developed in pelitic gneiss layers. Axial planar foliation (S_{m-1}) developed at the hinge of tight F_{m-1}. b) Boudinage of thin layers of hornblende-biotite mafic gneiss. Note that intervening parts are filled with leucocratic rock continuous with adjacent felsic layers. c) Boudinage of mafic layers and alignment of leucocratic seams oblique to compositional layers. d) Local development of axial planar foliation S_m at the hinge of an F_m fold. e) Alignment of leucocratic veins parallel to axial plane of an F_m fold. Note that a tight F_{m-1} fold with a core occupied by a grey thin felsic layer is refolded by F_m. f) Local development of upright open F_{m+1}. No axial planar foliation is present. An F_m fold is visible in the right side of the photograph.*
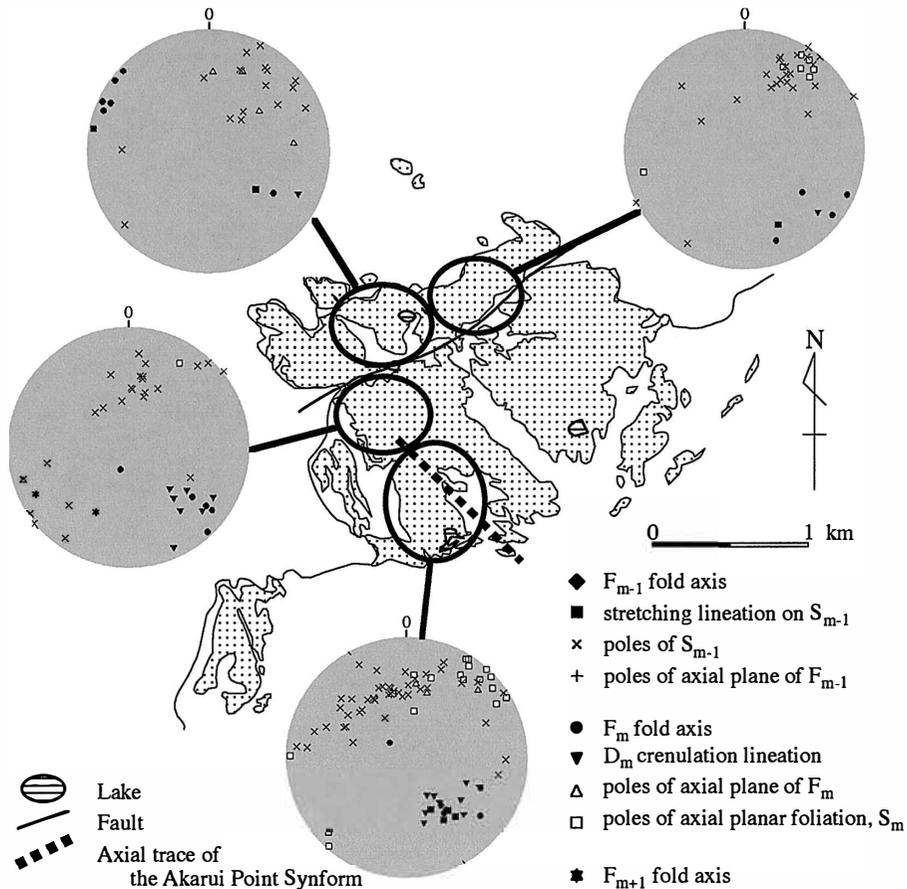
Fig. 3.   *Plots of structural data on Schmidt's nets, projected to the lower hemisphere.*

3.4.   Timing of the Akarui Point Synform

Figure 3 shows plots of structural data in four areas of Akarui Point, where data were collected from several outcrops in each area.   Two of the areas lie on the eastern limb of the Akarui Point Synform and the other two are located along the fold axis of the synform.   The orientation of S_{m-1} poles lies on a great circle with a pole that coincides with the orientation of F_m fold axes (Fig. 3).   No difference is detected between the areas in the eastern limb and the hinge of the synform.   Further, orientations of F_m axial planes consistently strike NW-SE with steep dips towards SW.   The deformation post-dating D_m, *i.e.*, D_{m+1}, is not responsible for the general orientation of structures in the area.   Considering these features along with the axial trend of the Akarui Point Synform, we conclude that the Akarui Point Synform was formed during D_m.

4. Chemical composition of biotite defining S_{m-1} and S_m

Two samples, #I-042 and #I-058A, were examined to detect differences in the chemical composition of biotite formed during D_{m-1} and D_m. Sample #I-042 is a relatively fine-grained biotite-hornblende mafic gneiss that was collected from the F_m hinge shown in Fig. 2d.   The sample contains S_{m-1} subparallel to compositional layers
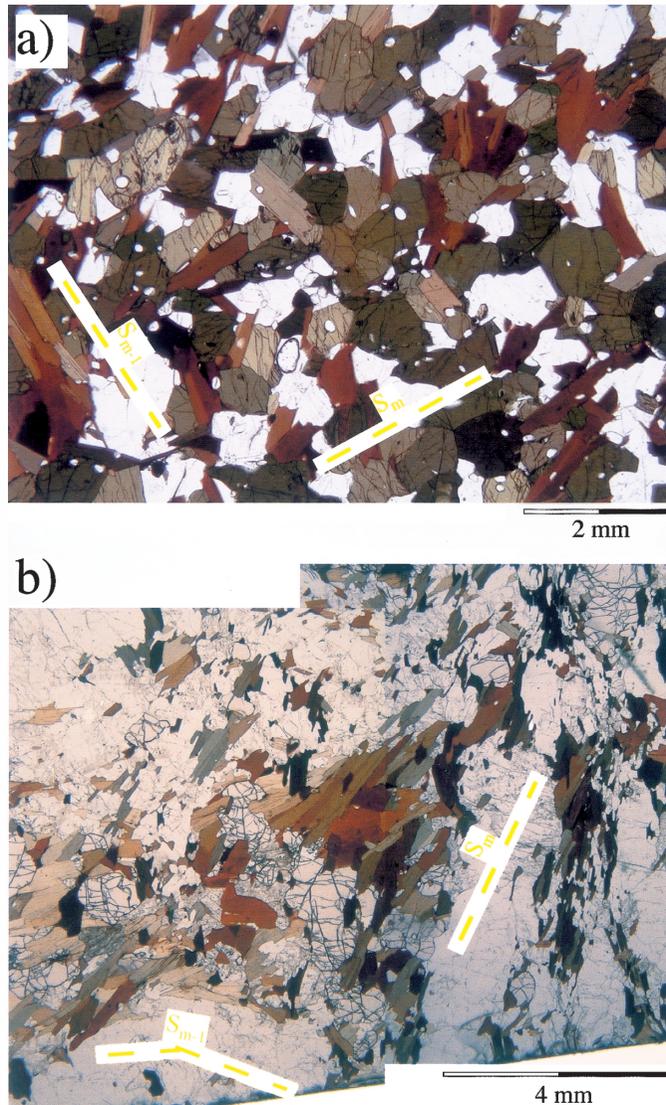

2 mm

4 mm

Fig. 4.   Photomicrographs showing occurrence of S_{m-1} and S_m at the hinge of F_m folds.
a) Biotite-hornblende mafic gneiss from outcrop shown in Fig. 2d (#I-042).
b) Garnet-biotite pelitic gneiss from near the outcrop of Fig. 2f (#I-058A).

together with S_m parallel to the axial plane of F_m. Both foliations are defined by the preferred orientation of biotite (Fig. 4a). Sample #I-058A is a garnet-biotite gneiss collected from the hinge of an F_m fold and contains biotite grains defining S_{m-1} parallel to compositional layers and S_m parallel to the axial plane of F_m (Fig. 4b).

The chemical compositions of biotite were determined using a scanning electron microscope (JEOL JSM-5800LV) combined with a Link ISIS analytical system at Kyushu University, under analytical conditions of 500 pA beam current, 20 kV accelerating voltage and 100 s count-times. Figure 5 shows the composition of biotite from the two samples with respect to Al *vs.* Mg/(Fe+Mg) and Si *vs.* Ti. Compositions of biotite defining each foliation are the same in both samples.
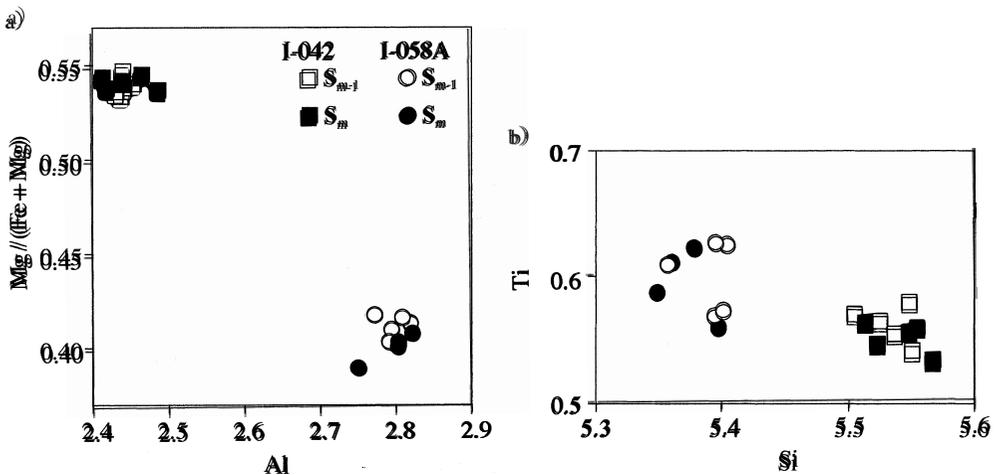

Fig. 5. *Chemical compositions of biotite from biotite-hornblende mafic (#I-042) and garnet-biotite pelitic (#I-058A) samples, based on 22 oxygens. Biotite grains are divided into two groups based on microscopic observation of association with S_{m-1} or S_m foliations.*

5. Discussion

5.1. *Temporal relations between deformation and metamorphism*

Akarui Point lies in the transitional zone between amphibolite-facies and granulite-facies metamorphism in the Lützow-Holm Complex. Temperatures as high as 750°C have been described in the lowest-grade part of the transitional zone at Tenmondai Rock (Hiroi *et al.*, 1983b). Hiroi *et al.* (1995) described the occurrence of euhedral and calcic plagioclase inclusions in garnet, indicative of partial melting in the lowest-grade part of the complex at Sinnan Rocks. These features suggest that the rocks at Akarui Point underwent metamorphism at temperatures above that of dehydration melting of muscovite in the granitic system (*e.g.*, Johannes and Holtz, 1996). The leucocratic veins that occur along the axial planes of both F_{m-1} and F_m (Fig. 2c, e), and fill the intervals between boudins formed during D_{m-1} (Fig. 2b) may, therefore, represent the
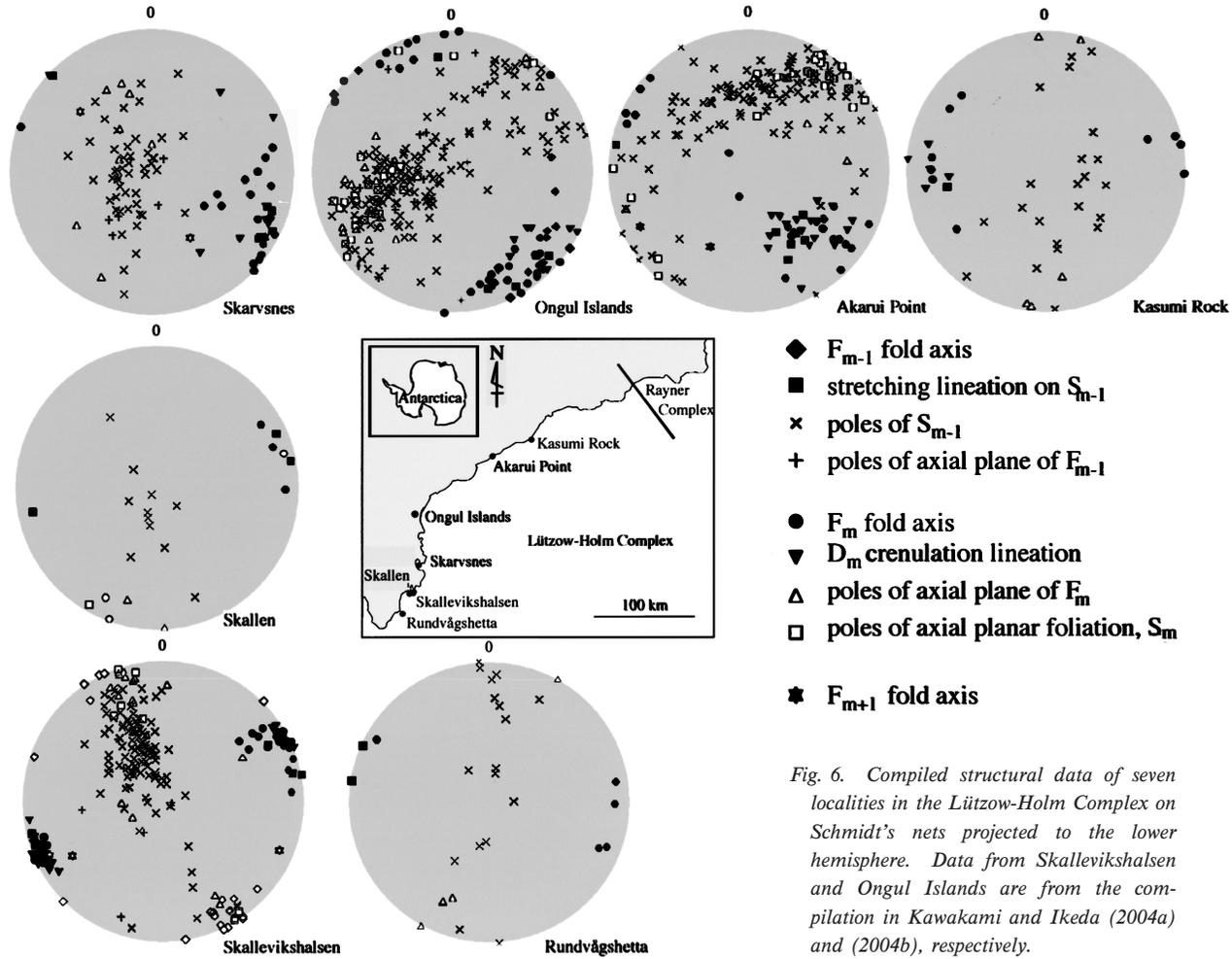
Fig. 6. Compiled structural data of seven localities in the Lützow-Holm Complex on Schmidt's nets projected to the lower hemisphere. Data from Skallevikshalsen and Ongul Islands are from the compilation in Kawakami and Ikeda (2004a) and (2004b), respectively.

former presence of melt, suggesting that high-temperature conditions continued during D_{m-1} and D_m. The identical compositions of biotite defining S_{m-1} and S_m could be explained in different ways: chemical homogenization at high temperatures during D_m; similar temperature conditions during D_{m-1} and D_m, and/or the rotation of biotite grains defining S_{m-1} into S_m. The last interpretation assumes plastic deformation of surrounding minerals, which also requires relatively high temperatures. Therefore, all three interpretations are consistent with the above conclusion.

Even though the metamorphic conditions during D_{m+1} are poorly constrained, neither axial planar foliation at the hinge of F_{m+1} folds nor leucocratic veins contemporaneous to the formation of D_{m+1} structures were recognized, suggesting that D_{m+1} took place at lower temperatures than D_{m-1} and D_m.

5.2. Overview of the structural features of the Lützow-Holm Complex

Shiraishi *et al*. (1983) traced lithologic boundaries through the Lützow-Holm Complex, and pointed out that the modes and phases of deformation along the Prince Olav Coast are similar to those in Lützow-Holm Bay. They also discussed the temporal relations between the phase of deformation and the peak of metamorphism. During JARE-44, deformation structures were investigated at Akarui Point, Skallevikshalsen (Kawakami and Ikeda, 2004a) and the Ongul Islands (Kawakami and Ikeda, 2004b), as well as at Kasumi Rock, Skarvsnes, Skallen and Rundvågshetta. Compiling structural data from these areas, we overview here the structural features of the Lützow-Holm Complex from the lowest-grade to approximately highest-grade areas (Fig. 6), and evaluate the validity of interpretations in Shiraishi *et al*. (1983).

In each locality in Fig. 6, identification of deformation stage is the same as that at the Akarui Point. Figure 6 shows that the orientation of compositional layers and foliations subparallel to them (S_{m-1}) in each locality is controlled by F_m, since F_m axes are parallel to the pole of a great circle defined by the variation in S_{m-1} poles. In addition, the orientations of F_m axes accord with the axial traces of macroscopic folds in most localities (Yoshida *et al*., 1976; Hiroi *et al*., 1983c; Nishida *et al*., 1984; Yanai *et al*., 1984; Motoyoshi *et al*., 1986). Based on these features, we consider that the folds described in the geological maps correspond mostly to F_m, and that F_m corresponds to F_1 of Shiraishi *et al*. (1983).

The F_m axial traces were folded by folds with axes subparallel to F_m in the Ongul Islands (M. Ishikawa *et al*., 1994) and highly oblique to F_m in Skarvsnes (T. Ishikawa *et al*., 1977). The orientation of F_m in Skarvsnes shows significant variation (Fig. 6). Furthermore, the orientations of D_m structures vary considerably across the Lützow-Holm Complex (Fig. 6). However, the orientations of D_{m+1} structures at Akarui Point are not consistent with the change in strike of subvertical S_m across the complex. Another as yet unrecognized phase of deformation may account for these features.

Shiraishi *et al*. (1983) considered that D_1 (D_m of this study) was contemporaneous with the peak of metamorphism, based mainly on the parallelism of mineral lineations and major fold axes. However, recent studies have revealed that even D_{m-1} occurred after peak metamorphism (*e.g*., Kawakami and Motoyoshi, 2004; Kawakami and Ikeda, 2004b). By taking the clockwise nature of the *P-T* path into account, it is likely that D_{m-1} and D_m took place during the exhumation of the complex.

6. Conclusions

The structural analysis of the Lützow-Holm Complex at Akarui Point and the compilation of structural data from lowest- to highest-grade localities of the complex lead to the following conclusions. Three phases of deformation are recognized at Akarui Point, and are referred to as D_{m-1}, D_m and D_{m+1} in temporal order. D_{m-1} produced a foliation composed of biotite and hornblende subparallel to compositional layers and locally axial planar to isoclinal and intrafolial folds. D_{m-1} also produced boudins with long axes subparallel to the axes of F_{m-1}. The D_m phase corresponds to the development of crenulation and axial planar foliations that trend NE-SW throughout the area. The large scale Akarui Point Synform has an axis that plunges gently SE, and is attributed to D_m. D_{m+1} structures involve a gentle folding without formation of a foliation. The first two phases of deformation are closely associated with the segregation of melt veins and the formation of biotite of consistent composition. These features suggest that the first two phases of deformation took place at temperatures above that of dehydration melting of muscovite in the granitic system.

The D_{m-1} and D_m phases took place throughout the complex at high temperatures during exhumation. This conclusion stresses the importance of characterizing D_{m-1} and pre-D_{m-1} structures to elucidate the metamorphic evolution of the Lützow-Holm Complex.

Acknowledgments

References

Fraser. G., McDougall, I., Ellis, D.J. and Williams, I.S. (2000): Timing and rate of isothermal decompression in Pan-African granulites from Rundvågshetta, East Antarctica. J. Metamorph. Geol., **18**, 441–454.

Hiroi, Y., Shiraishi, K., Nakai, Y., Kano, T. and Yoshikura, S. (1983a): Geology and petrology of Prince Olav Coast, East Antarctica. Antarctic Earth Science, ed. by R.L. Oliver *et al*. Canberra, Aust. Acad. Sci., 32–35.

Hiroi, Y., Shiraishi, K., Yanai, K. and Kizaki, K. (1983b): Aluminum silicates in the Prince Olav and Sôya Coasts, East Antarctica. Mem. Natl Inst. Polar Res., Spec. Issue, **28**, 115–131.

Hiroi, Y., Shiraishi, K. and Yoshida, Y. (1983c): Geological map of Sinnan Rocks, Antarctica. Antarct. Geol. Map Ser., Sheet 14 (with explanatory text 7 p.). Tokyo, Natl Inst. Polar Res.

Hiroi, Y., Shiraishi, K., Motoyoshi, Y., Kanisawa, S., Yanai, K. and Kizaki, K. (1986): Mode of occurrence, bulk chemical compositions, and mineral textures of ultramafic rocks in the Lützow-Holm Complex, East Antarctica. Mem. Natl Inst. Polar Res., Spec. Issue, **43**, 62–84.

Hiroi, Y., Shiraishi, K., Motoyoshi, Y. and Katsushima, T. (1987): Progressive metamorphism of calc-silicate rocks from the Prince Olav and Sôya Coasts, East Antarctica. Proc. NIPR Symp. Antarct. Geosci.,

1, 73–97.

Hiroi, Y., Motoyoshi, Y., Shiraishi, K. and Ellis, D.J. (1995): The significance of euhedral calcic plagioclase inclusions in garnet from the Lützow-Holm Complex, East Antarctica: A textural indicator of partial melting in pelitic gneisses. Proc. NIPR Symp. Antarct. Geosci., **8**, 107–120.

Hiroi, Y., Motoyoshi, Y., Ellis, D.J., Shiraishi, K. and Kondo, Y. (1997): The significance of phosphorus zonation in garnet from high-grade pelitic rocks: A new indicator of partial melting. The Antarctic Region: Geological Evolution and Processes, ed. by A.C. Ricci. Siena, Terra Antarct. Publ., 73–77.

Ishikawa, M., Shiraishi, K., Motoyoshi, Y., Tsuchiya, N., Shimura, T. and Yanai, K. (1994): Geological map of Ongul Islands, Antarctica. Antarct. Geol. Map Ser., Sheet 36 (with explanatory text 21 p.). Tokyo, Natl Inst. Polar Res.

Ishikawa, T., Yanai, K., Matsumoto, Y., Kizaki, K., Kojima, S., Tatsumi, T., Kikuchi, T. and Yoshida, M. (1977): Geological map of Skarvsnes, Antarctica. Antarct. Geol. Map Ser., Sheet 6 and 7 (with explanatory text 10 p.). Tokyo, Natl Inst. Polar Res.

Johannes, W. and Holtz, F. (1996): Petrogenesis and Experimental Petrology of Granitic Rocks. Berlin, Springer, 335 p.

Kawakami, T. and Ikeda, T. (2004a): Timing of ductile deformation and peak metamorphism in Skallevikshalsen, Lützow-Holm Complex, East Antarctica. Polar Geosci., **17**, 1–11.

Kawakami, T. and Ikeda, T. (2004b): Structural evolution of the Ongul Islands, Lützow-Holm Complex, East Antarctica. Polar Geosci., **17**, 12–21.

Kawakami, T. and Motoyoshi, Y. (2004): Timing of attainment of spinel+quartz coexistence in the garnet-sillimanite leucogneiss from Skallevikshalsen, Lützow-Holm Complex, East Antarctica. J. Mineral. Petrol. Sci., **99** (in press).

Motoyoshi, Y. and Ishikawa, M. (1997): Metamorphic and structural evolution of granulites from Rundvågshetta, Lützow-Holm Bay, East Antarctica. The Antarctic Region: Geological Evolution and Processes, ed. by C.A. Ricci. Siena, Terra Antarct. Publ., 65–72.

Motoyoshi, Y., Matsueda, H., Matsubara, S., Sasaki, K. and Moriwaki, K. (1986): Geological map of Rundvågskollane and Rundvågshetta, Antarctica. Antarct. Geol. Map Ser., Sheet 24 (with explanatory text 11 p.). Tokyo, Natl Inst. Polar Res.

Motoyoshi, Y., Matsubara, S. and Matsueda, H. (1989): *P-T* evolution of the granulite-facies rocks of the Lützow-Holm Bay region, East Antarctica. Evolution of Metamorphic Belts, ed. by J.S. Daly *et al*. Oxford, Geol. Soc., 325–329 (Geol. Soc. Spec. Publ. 43).

Nishida, T., Yanai, K., Kojima, H., Matsueda, H. and Kanisawa, S. (1984): Geological map of Kasumi Rock, Antarctica. Antarct. Geol. Map Ser., Sheet 18 (with explanatory text 6 p.). Tokyo, Natl Inst. Polar Res.

Shiraishi, K., Hiroi, Y., Sasaki, K., Yanai, K. and Kizaki, K. (1983): Geological structure of the Prince Olav Coast. The 4th Symposium on Antarctic Geosciences, Program and Abstracts, 28–29 October 1983. Tokyo, Natl Inst. Polar Res., 79–80 (in Japanese).

Shiraishi, K., Hiroi, Y. and Onuki, H. (1984): Orthopyroxene-bearing rocks from the Tenmondai and Naga-iwa Rocks in the Prince Olav Coast, East Antarctica: First appearance of orthopyroxene in progressive metamorphic sequence. Mem. Natl Inst. Polar Res., Spec. Issue, **33**, 126–144.

Shiraishi, K., Hiroi, Y., Motoyoshi, Y. and Yanai, K. (1987): Plate tectonic development of Late Proterozoic paired metamorphic complexes in eastern Queen Maud Land, East Antarctica. Gondwana Six: Structure, Tectonics, and Geophysics, ed. by G.W. McKenzie. Washington, D.C., Am. Geophys. Union, 309–318 (Geophys. Monogr. 40).

Shiraishi, K., Hiroi, Y., Ellis, D.J., Fanning, C.M., Motoyoshi, Y. and Nakai, Y. (1992): The first report of a Cambrian orogenic belt in East Antarctica—An ion microprobe study of the Lützow-Holm Complex. Recent Progress in Antarctic Earth Science, ed. by Y. Yoshida *et al*. Tokyo, Terra Sci. Publ., 67–73.

Shiraishi, K., Ellis, D.J., Hiroi, Y., Fanning, C.M., Motoyoshi, Y. and Nakai, Y. (1994): Cambrian orogenic belt in East Antarctica and Sri Lanka: implications for Gondwana assembly. J. Geol., **102**, 47–65.

Yanai, K., Kizaki, K., Shiraishi, K., Hiroi, Y. and Kanisawa, S. (1984): Geological map of Akarui Point and Naga-iwa Rock, Antarctica. Antarct. Geol. Map Ser., Sheet 20 (with explanatory text 6 p.). Tokyo, Natl Inst. Polar Res.

Yoshida, M. (1978): Tectonics and petrology of charnockites around Lützow-Holmbukta, East Antarctica. J. Geosci., Osaka City Univ., **21**, 65–152.

Yoshida, M., Yoshida, Y., Ando, H., Ishikawa, T. and Tatsumi, T. (1976): Geological map of Skallen, Antarctica. Antarct. Geol. Map Ser., Sheet 9 (with explanatory text 16 p.). Tokyo, Natl Inst. Polar Res.

Yoshimura, Y., Motoyoshi, Y., Miyamoto, T., Grew, E.S., Carson, C.J. and Dunkley, D.J. (2004): High-grade metamorphic rocks from Skallevikshalsen in the Lützow-Holm Complex, East Antarctica: Metamorphic conditions and possibility of partial melting. Polar Geosci., **17**, 57–87.